Formation of unusual yellow Orapa diamonds

Timmerman, Suzette; Chinn, Ingrid L.; Fisher, David; Davies, Gareth R.

published in
Mineralogy and Petrology
2018

DOI (link to publisher)
10.1007/s00710-018-0592-9

document version
Publisher's PDF, also known as Version of record

Mineralogy and Petrology (2018) 112 (Suppl 1):S209–S218
https://doi.org/10.1007/s00710-018-0592-9

ORIGINAL PAPER

Formation of unusual yellow Orapa diamonds

Suzette Timmerman[1] · Ingrid L. Chinn[2] · David Fisher[3] · Gareth R. Davies[1]

Received: 14 November 2017 / Accepted: 11 May 2018 / Published online: 21 June 2018

Abstract

Twenty eclogitic diamonds from Orapa Mine (Botswana) with an unusual yellow colour are characterised for their growth structure, N systematics, and C isotope composition, and the major element composition of their silicate inclusions. The diamonds show complex luminescence with green, blue and non-luminescent zones and occasional sector zonation. All parts of the diamonds have low total N concentrations (<50 at.ppm, with one exception of <125 at.ppm) and a limited range in C isotope composition (−5.7 to −10.6‰). Fourier Transform Infrared spectra show bands at 1334, 1332, 1282, and 1240 cm^{-1} typical for Ib-IaA diamonds. Relict unaggregated N defects (N_s^o and N_s^+) are present and the preservation is likely caused by the low N concentrations and possible low mantle residence temperatures rather than young diamond formation (inclusion ages of 140, 1096, 1699 Ma; Timmerman et al. Earth Planet Sc Lett 463:178–188, 2017). Garnet and clinopyroxene inclusions extracted from 14 diamonds have an eclogitic composition with relatively low Ca contents and based on all characteristics, these diamonds form a distinct population from Orapa.

Keywords Carbon isotopes · Nitrogen · Silicate inclusions · Zimbabwe Craton

Introduction

Compositional data of fluid inclusions (e.g. Navon et al. 1988; Schrauder and Navon 1994; Klein-BenDavid et al. 2004) in fibrous diamonds indicate that these diamonds formed from volatile-rich fluids moving through the sub-continental lithospheric mantle. Carbon isotope ratios ($\delta^{13}C_{VPDB}$) and N content of the diamond host and major and trace elements of mineral inclusions also provide information on the origin of the fluid responsible for diamond formation and the growth environment. The complex growth structures in monocrystalline diamonds associated with coupled changes in N content, aggregation state, and/or $\delta^{13}C_{VPDB}$ reflect episodic diamond growth and changes in the C-H-O-S rich diamond-forming media (Shirey et al. 2013 and references therein, Wiggers-de Vries et al. 2013a, Petts et al. 2016). Previous research on diamonds from the Orapa Mine (Botswana) established that the $\delta^{13}C_{VPDB}$ for eclogitic diamonds of DTC sieve class −7 + 5 ranges from −2.6 to −18.0‰ with generally high bulk N contents (range of 24–1352 at.ppm total N; Deines et al. 1993; Cartigny et al. 1999). Despite a wide range in chemical compositions of the mineral inclusions (Gurney et al. 1984), a limited range of formation temperatures is associated with mineral inclusions of Orapa diamonds with $\delta^{13}C_{VPDB} <$ −8‰ (Deines and Harris 2004).

In the past decades a variety of diamonds with different colours and morphologies were investigated to better understand mantle processes and diamond formation. Previous research on the Orapa diamond mine was performed on eclogite xenoliths and on peridotitic and eclogitic diamonds by Deines et al. (1991), Cartigny et al. (1999), Stachel et al. (2004), Deines and Harris (2004), and Deines et al. (2009). For Orapa, Shee (1978) reported dominantly eclogitic xenoliths, but more recent studies of xenoliths recovered from the open pit and drill cores suggest that eclogite makes up only 10% of the xenolith population (Meulemans et al. 2012). The mineral inclusions in Orapa diamonds are dominated by sulphides

Editorial handling: T. Stachel

Electronic supplementary material The online version of this article (https://doi.org/10.1007/s00710-018-0592-9) contains supplementary material, which is available to authorized users.

✉ Suzette Timmerman
suzette.timmerman@anu.edu.au

[1] Vrije Universiteit, De Boelelaan 1085, 1081 HV Amsterdam, The Netherlands

[2] De Beers Exploration, Private Bag X01, Southdale 2135, Johannesburg, South Africa

[3] De Beers Technologies, Belmont Road, Maidenhead SL6 6JW, UK

(73%), followed by eclogitic silicates (19%) and peridotitic silicates (8%) (Gress et al. 2017).

It is important to build an understanding of the number and nature of diamond formation events in the mantle beneath specific localities to understand how diamond genesis varies in space and time. This study focuses on determining the specific characteristics of a previously undocumented eclogitic diamond sub-population at the Orapa mine to establish if it represents a diamond-forming event under distinct conditions. The yellow colour of the studied diamonds has a different appearance to the more common "Cape yellow" colour. The Cape yellow colour is caused by high N3/N2 abundances and absorption of light by the N3V defect, which consists of three N atoms and a vacancy (Fritsch 1998). The studied diamonds have an uneven yellow colour owing in part to the presence of relict unaggregated N defects (single nitrogen (N_s^0 and N_s^+) defects). For more information the reader is referred to King et al. (2005) for specific detail regarding defects in yellow diamonds. Recent changes to processing at Orapa have significantly increased the yield of these unusual yellow diamonds. The diamonds studied were sizeable; ¾ to 1 carat (1 carat = 200 mg), underlining the economic importance of understanding the formation of these particular diamonds. To this end, we present a detailed Fourier-transform infrared spectroscopy (FTIR), carbon isotope and inclusion major element study of 20 of these previously undocumented eclogitic diamonds from Orapa. A previous study by Timmerman et al. (2017) on the same diamonds focused on trace element compositions and Rb-Sr and Sm-Nd isotope systematics of nine silicate inclusions.

Methods

Preparation and luminescence imaging

The diamonds were windowed or laser cut, where visible along the 110 crystallographic orientation, into ~0.5–2 mm thick plates and polished along the cut faces at De Beers Technology Centre, Maidenhead. The luminescence zonation of the diamond plates was examined on both sides with a DiamondView™ instrument that uses short wavelength UV light (<230 nm) to excite luminescent defects of the diamonds. The luminescence emitted by the diamonds was imaged with a solid-state charge-coupled device (CCD) video camera (Welbourn et al. 1996). FTIR analyses were performed on the polished plates, before the diamonds were broken to extract the inclusions for electron probe micro-analyses (EPMA). Growth zones of the diamonds were coloured with permanent markers prior to breakage allowing recovery of fragments from different zones for C isotope analyses.

FTIR analyses

High resolution infrared spectra were taken for each sample over the range 7000 to 400 cm^{-1} at a resolution of 0.5 cm^{-1} with a Thermo Scientific Nicolet iS50 FTIR spectrometer at De Beers Technology Centre, Maidenhead. The presence of N_s^0 was identified in these high resolution spectra and concentrations were calculated, after normalisation to 1 cm diamond thickness and baseline correction, using a conversion factor of 1.4×25 (Kiflawi et al. 1994 and unpublished experimental data from D. Fisher; this conversion factor is close to results from Liggins 2010). Subsequently, infrared spectra were measured in different growth zones of the polished diamond plates using a FT/IR Jasco-470 plus spectrometer equipped with a Jasco Irtron IRT-30 infrared microscope at the Utrecht University. Transmission spectra were collected over the range 4000–650 cm^{-1} at a resolution of 4 cm^{-1} with 200 scans per spectrum. After baseline correction, the data were normalized to 1 cm diamond thickness with an absorption coefficient of 11.94 at 1995 cm^{-1}, and a Type IIa spectrum was subtracted (Mendelssohn and Milledge 1995).

Carbon isotope analyses

Different growth zones were recognized based on changes in luminescence intensities and colours. Carbon isotope analyses were performed on 30–100 μg fragments of different growth zones from 17 diamonds using a Carlo Erba NC 2500 element analyser coupled to a Thermo Finnigan Delta Plus stable isotope ratio mass spectrometer (SIRMS). The samples were compared to two reference gas peaks that were calibrated against V-PDB and are expressed in the conventional per mil notation. This delta expression was corrected for any potential instrumental bias by measuring the external standards USGS24 (−16.05‰) and VICS (+1.35‰) and any drift of the instrument was monitored with two internal standards WK (−7.16‰, Wiggers-de Vries et al. 2013, synthetic diamond powder) and PC (−8.22‰, natural diamond powder provided by P. Cartigny of the Institut de Physique du Globe de Paris). The analyses had an external reproducibility of 0.2‰ 2SE based on repeat analyses of standards, while the internal precision was better than 0.1‰.

EPMA analyses

The mineral inclusions were measured unpolished on a Jeol JXA-8800 M electron probe microanalyzer using a beam size of 1 μm with a beam current of 25 nA and an acceleration voltage of 15 kV. Multiple analyses were taken on each mineral and analyses with <90 wt% totals and outside two standard deviations of the average for major elements and stoichiometry were rejected, as tilted surfaces can affect the analysis. Analyses with a nonideal stoichiometry (<3.9 or > 4.1 cations per 6 oxygen) are also rejected. After rejection of outliers and normalisation to 100%, data generally lie within 1% (relative)

for major element (oxide concentration > 1.5 wt%) analyses of the same minerals after polishing and thus can be reliably used to distinguish different types of garnet or clinopyroxenes (Timmerman et al. 2015). On average the precision is 1.3× worse compared to results of polished minerals. More details on standards, spectrometer set-up, accuracy and reproducibility can be found in Timmerman et al. (2015). The minerals were measured unpolished to preserve as much material as possible for subsequent isotope analyses.

Results

Description

The twenty diamonds studied from Orapa were mined in 2012. Photographs and DiamondView™ luminescence images of one side of the diamond plates OR13, OR15, and OR19 are shown as examples in Fig. 1. Images of the rough samples are provided in electronic supplementary material 1 and DiamondView™ images of both sides of the polished plates are provided in electronic supplementary material 2 for the samples not reported in Timmerman et al. (2017).

In general, all the diamonds have uneven yellow to orange colours and have an irregular octa-dodecahedral morphology (Electronic supplementary material 1), with trigons present on some faces (Table 1). The diamonds range from 0.33–1.23 carats (average 0.71 carats). The internal growth structure of central plates, as revealed by DiamondView™ luminescence imaging, shows complex intergrowth of zones with green, blue and non-luminescent zones. Growth sector zonation was identified in the green luminescent zones that are directly related to the yellow/orange colour in normal transmitted light (Fig. 1). The growth sector zonation is clearly identified in the DiamondViewTM images of diamonds OR04, OR08, OR09, OR13, OR15, and OR19 (Fig. 1; Electronic supplementary

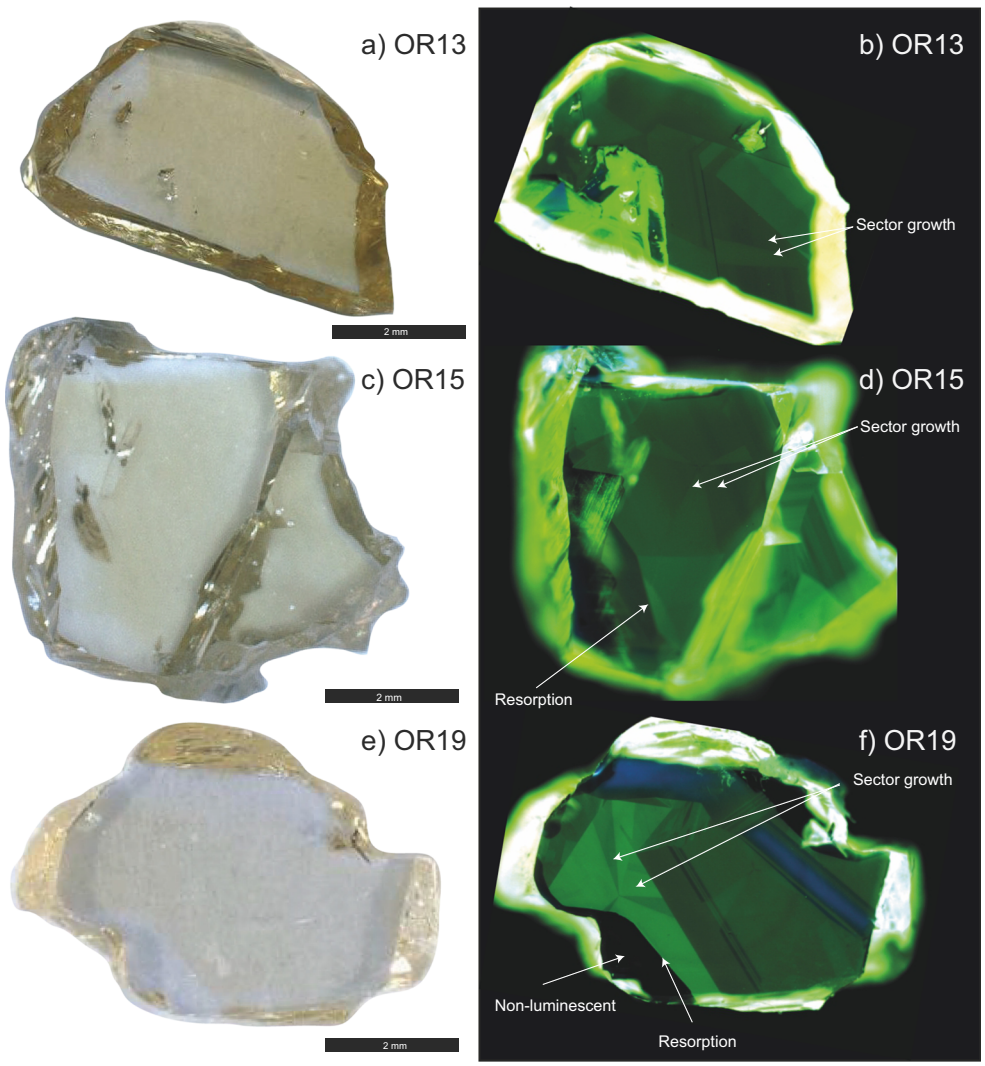

Fig. 1 Normal reflected light images (**a**, **c**, **e**) and DiamondView™ luminescent images (**b**, **d**, **f**) of diamonds OR13, OR15, and OR19, showing the relation of the yellow colour in reflected light to the green luminescent area in DiamondView™

Table 1 Diamond description and relict nitrogen content and carbon isotope characteristics

Sample	Weight (mg)	Type[a]	Inclusions[b]	Colour[c]	Features	N_s^0 (ppm)[d]	$\delta^{13}C_{VPDB}$ (‰)[e] Inner 1	Inner 2	Inner 3	Outer 1	Outer 2	Outer 3
OR01	242	E	3 sf, 2 sil, grt	amber orange	trigons	0.4	−7.67	−7.4	–	−7.79	−9.57	–
OR02	246	E	11 grt, 1 cpx	un col yellow-orange		0.3	−10.38	−10.51	−10.56	−10.49	−10.36	–
OR03	200	E	2 cpx, 5 sil	un col yellow-orange	corrosion	0.4	−7.98	−8.21	–	−7.5	−7.5	–
OR04	189	E	1 cpx, 1 grt, 1 sf	amber orange	trigons	0.2	−8.58	–	–	−8.62	–	–
OR05	145	E	2 grt	orange	trigons, corrosion	0.5	−7.49	–	–	−7.61	–	–
OR06	164	E	6 grt, 2 cpx	un col orange		0.3	−7.12	–	–	−7.03	–	–
OR07	180	E	3 cpx, 2 grt	orange	trigons, shield-shaped laminae	0.4	−6.86	–	–	−6.61	−6.78	–
OR08	174	E	4 grt	orange	trigons	0.6	−6.12	−6.83	–	−8.11		–
OR09	134	E	1 grt, 1 cpx	yellow-orange	trigons	0.4	−7.82	−7.86	–	−7.55		–
OR10	65	E	5 grt	yellow-orange	tetragons	0.4	−8.8		–	−9.38	−7.5	–
OR11	92	S	11 sf	yellow-orange	trigons, hillocks, corrosion	0.2	–	–	–	–	–	–
OR12	77	E	4 grt, 3 sf	orange	smoothed faces	0.6	−2.93	−7.36	–	−6.81	−7.07	–
OR13	142	E	2 cpx, 4 grt	orange	trigons	0.5	−5.65	–	–	−7.96	−7.93	−8.02
OR14	169	S	3 sf, 1 sil	yellow	trigons, stepped faces	0.6	−8.1	–	–	−7.72	−7.99	–
OR15	145	S	2 sf	orange		0.6	–	–	–	–	–	–
OR16	78	S	sf	orange	stepped faces	0.4	–	–	–	–	–	–
OR17	94	E	cpx	orange	smoothed faces	0.4	−6.54	–	–	−6.67	−6.55	−6.79
OR18	116	E	grt, 5 cpx	orange	trigons	0.4	−8.95	−8.63	–	−8.85	−7.46	–
OR19	79	S	2 sf, 1 sil	yellow	frosted surface	1.1	−9.16	−8.9	−8.45	−9.34	–	–
OR20	104	E	5 grt	orange	tetragons	0.9	−7.9	–	–	−7.98	–	–

[a] Type: paragenesis with E for eclogitic and S for diamonds with sulphides but no distinguishing silicate inclusions

[b] Inclusions: grt = garnet, cpx = clinopyroxene, sf = sulphide, sil = unidentified silicate

[c] Colour: un col. = uneven coloured

[d] N_s^0 is neutral single nitrogen based on the spectra with 0.5 cm^{-1} resolution

[e] Diamonds OR11, OR15, and OR16 were not measured. Number of measurements in inner and outer growth zones numbered 1–3 per growth zone. Images of the growth zones can be seen in Fig. 1 and Electronic supplementary material 2 and Timmerman et al. (2017)

material 2; Supplementary information of Timmerman et al. 2017). The green luminescent zones form the bulk of the innermost major growth zones and these zones are sometimes associated with multiple (up to 6) thin (50–300 μm) blue luminescent layers (e.g. OR12; Electronic supplementary material 2). These major growth zones are always resorbed and have a low to non-luminescent layer directly in contact with the resorption surface before any subsequent outer blue growth zones (Fig. 1, Electronic supplementary material 2). The lack of luminescence is caused by low nitrogen concentrations and presence of A-centre defects that can quench luminescence (A-centres are <30–50 at.ppm, except for diamond OR02). Eight of the twenty diamonds studied show a blue luminescent growth zone in the outer region comprising between 1 and 8 fine layers. The non-luminescent to blue zones correspond to colourless zones in transmitted light.

FTIR spectra

FTIR spectra of both resolutions (0.5 and 4 cm^{-1}) show that all growth zones are characterised by low total N concentrations (<50 at.ppm, except for OR02 with <120 at.ppm; Fig. 2a). Bands are present at 1334 (N_s^0; Fig. 2b), 1332 (N_s^+, D, and other defects), 1282 (A + B), and 1240 cm^{-1} (characteristic for Ib-IaA diamonds; Collins and Mohammed 1982; Woods and Collins 1983). In some cases, there is a platelet band at ~1370 cm^{-1} and a weak band at 1175 cm^{-1} (B; Electronic supplementary material 3). The band observed at 1332 cm^{-1} in FTIR spectra is not as well-defined as in previous studies where it was interpreted as X-centres/N_s^+ (Lawson et al. 1998; Zedgenizov et al. 2016). Thus the N_s^+ concentrations are lower than in previous studies and/or other defects play a role in causing this band. Y-centres at 1140–1150 cm^{-1}, previously found in some Ib diamonds (Hainschwang et al. 2012; Zedgenizov et al. 2016), were not detected. Generally, the single phonon region of the spectrum cannot be modelled by N_s^0, A-centre, and N_s^+ components alone. The nature of the defects causing the additional absorption is presently unknown and induces large uncertainties in estimates of the concentrations of the A and B components. Furthermore, due to the thickness of the plates, the transmission spectra represent a mix of both yellow and colourless zones of the diamonds. Therefore, N aggregation states could not be calculated precisely. Maximum A-centre N concentrations were estimated based on the band height at 1282 cm^{-1} using a conversion factor of 16.5 (Boyd et al. 1994) (Fig. 2; Electronic supplementary material 4); after normalisation to 1 cm diamond thickness. In general, the Orapa diamonds under study have consistently low N abundances (maximum A-centres <30–50 at.ppm, except for OR02), with slightly higher band heights at 1282 cm^{-1} in the colourless outer zones for diamonds OR02 and OR10 (Fig. 2c, d; Electronic supplementary material 4). Relict unaggregated N defects are present in all diamonds (Electronic supplementary

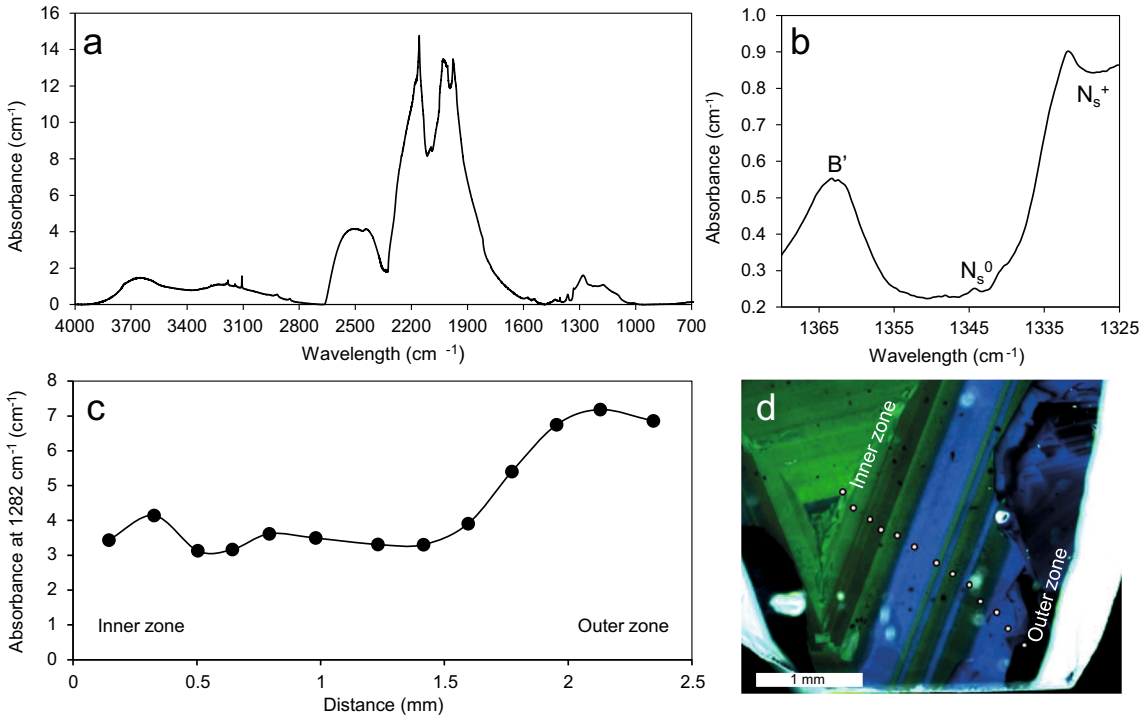

Fig. 2 **a** High resolution (0.5 cm^{-1}) FTIR spectrum of diamond OR07, showing the VN_3H at 3107 cm^{-1}, and low N contents (A-centre at 1282 cm^{-1}) relative to the diamond absorption. No Type II spectrum is subtracted from this spectrum to show the low N bands compared to the diamond absorbance bands. **b** 1363 (platelet/B′), 1344 (N_s^0) and 1332 cm^{-1} (partially caused by N_s^+) bands of the high-resolution spectrum (0.5 cm^{-1}) of diamond OR07. **c** 1282 cm^{-1} band height in absorbance per cm from the inner to outer zone of diamond OR02. The A-centre at 1282 cm^{-1} does not produce a visible colour in normal light. **d** measurement locations on diamond OR02 of the results shown in **c**

material 3). The 1344 cm^{-1} band from single substitutional N is very small. The 0.5 cm^{-1} resolution spectra were used to calculate N_s^0 concentrations with the band height at 1344 cm^{-1} and a conversion factor of 1.4 × 25 (Kiflawi et al. 1994 and unpublished experimental data from D. Fisher) and yield 0.2 to 1.1 at.ppm N_s^0 (Table 1, Fig. 2b). Some mixed spectra contain platelet bands, recording aggregation from A to B centres, most likely from the colourless growth zones.

All FTIR spectra record the presence of H defects with bands at 1405 cm^{-1} (C-H bending), 3000–3900 cm^{-1} (band maxima at around 3190 and 3650 cm^{-1}), and 3107 cm^{-1} (C-H stretch at VN_3H; Goss et al. 2014). A small carbonate band at ~1430 cm^{-1} is present in diamonds OR01, 02, 03, 05, 07, 08, 09, 12, 13, 14, 15, likely caused by submicron carbonate inclusions.

Carbon isotope composition

The $\delta^{13}C_{VPDB}$ values of the yellow Orapa diamonds show a restricted range of −2.9 to −10.6‰ with an average of −7.9 ± 1.3 (1SD), which falls within the mantle range of −1 to −10‰ (Kirkley et al. 1991). The yellow inner and colourless outer zones have a similar variation in carbon isotope composition of −5.7 to −10.6‰ and − 6.8 to −10.4‰ respectively (Table 1). One more ^{13}C enriched composition of −2.9‰ was found in the innermost zone (blue luminescence) of diamond OR12. Most diamonds record insignificant variation in their carbon isotope values from inner to outer zones. Three diamonds (OR03, OR10, OR18), however, have higher $\delta^{13}C_{VPDB}$ values in the outer zones, while three other diamonds (OR01, OR08, OR13) have lower $\delta^{13}C_{VPDB}$ values in the outer zones. Changes in $\delta^{13}C_{VPDB}$ values in these diamonds varied from 0.5 to 2.4‰ (Fig. 3).

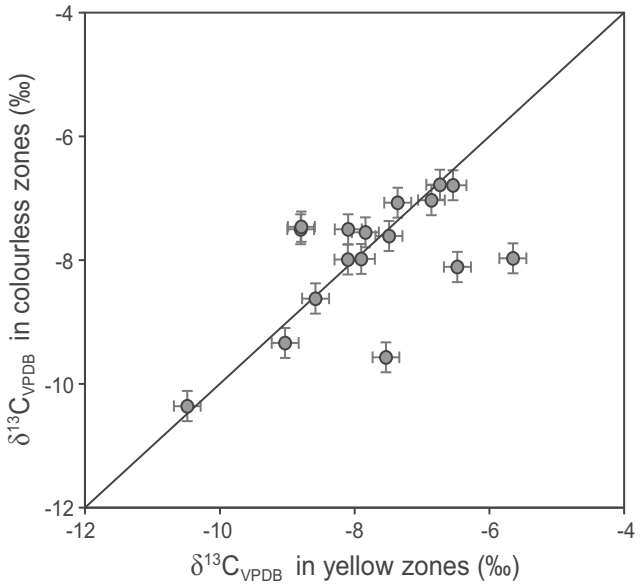

Fig. 3 Average C isotope compositions ($\delta^{13}C_{VPDB}$) determined on co-existing yellow and colourless zones of 17 diamonds

Major elements of garnet and clinopyroxene inclusions

All the mineral inclusions that were measured belong to the eclogitic suite (low Cr#), but none was recovered from the anomalous yellow body coloured zones associated with the relict unaggregated nitrogen. Silicate inclusions consisted of garnets, clinopyroxenes, and one mineral with the composition and stoichiometry of titanite (Table 2). Garnet inclusions show a limited range in CaO content of 3.5–6.1 wt%, with one CaO-poor outlier of 1.7 wt% (Fig. 4a). Both CaO and FeO decrease with increasing MgO content and the data form a single trend in bi-variant diagrams suggesting that there are no significantly different garnet populations in the studied diamonds. The MgO content (13.4–18.7 wt%) is higher than previously reported from garnets from diamonds from the Orapa kimberlite cluster (average of 11.8 ± 2.1 wt%; Gurney et al. 1984; Deines et al. 1993 and 11.4 ± 2.7 wt% for Letlhakane; Deines and Harris 2004). The clinopyroxene inclusions have oxide contents generally within the range found previously for Orapa and Letlhakane (Deines and Harris 2004), but have relatively higher MgO contents for the amount of Na_2O (Fig. 4b). Some significant compositional differences do exist within the silicate inclusions of this new diamond suite. Diamonds OR18 and OR08 contained a clinopyroxene outside the range of the other clinopyroxenes, suggesting that there are different eclogitic clinopyroxene populations present in this yellow diamond suite. Based on the DiamondView™ images three non-touching garnet-clinopyroxene pairs (OR06–2 and 06–7, 07–1 and 07–7, 10–2 and 10–4) are considered to have formed in equivalent growth zones and hence to be in chemical equilibrium. Using the Fe-Mg exchange thermometer of Krogh (1988) and assuming a pressure of 5 GPa, these mineral pairs yield temperatures between 1080 and 1160 °C. These are approximate temperatures as the major element data are not as precise and accurate as from polished minerals. Inclusions OR06–7 and OR07–1 were previously dated at 1699 ± 340 Ma (Timmerman et al. 2017).

Discussion

Cause of unaggregated nitrogen

Nitrogen aggregates from single N atoms (N_s^0 and N_s^+) to N pairs (A-centres) to four N atoms around a vacancy (B-centres) (Evans and Qi 1982), and the aggregation rate is dependent on time, temperature and nitrogen concentration (Taylor et al. 1990). The aggregation from A to B-centres produces N3 as a side reaction, and the platelet related defects B′ and D are found in diamonds with B-centres (Clark and Davey 1984). The relict unaggregated single N defects present

Table 2 Major element composition of garnet and clinopyroxene inclusions and a titanite inclusion

Sample	Na_2O[a]	MgO	SiO_2	Al_2O_3	K_2O	CaO	TiO_2	FeO	MnO	Cr_2O_3	NiO	Total[b]	Cat (apfu)[c]
Garnet													
OR02-8	0.2	14.8	42.3	21.4	0	6.1	0.4	14.4	0.3	0.1	0	100.2	7.96
OR04–3	0.1	18.7	44.4	19.6	0	3.5	0.4	12.8	0.3	0.1	0	95.9	7.96
OR05–1	0.4	16.7	42.8	21.2	0.2	4.2	0.4	13.6	0.4	0.1	0	95.1	7.96
OR06–2	0.1	15.1	39.5	23.5	0	4.6	0.4	16.3	0.4	0	0	96.7	8.04
OR06–4	0.2	15.5	36.7	25.4	0	4.8	0.5	16.5	0.4	0.1	0	91.2	8.14
OR07–7	0.2	15.2	41.4	22.6	0	4.4	0.4	15.3	0.4	0.1	0	103.8	7.98
OR08–3	0.1	15.5	41.6	22.7	0	4.1	0.5	15	0.4	0.1	0	103.4	7.94
OR10–1	0.2	17.3	42.6	23.2	0	3.5	0.4	12.4	0.3	0.1	0	108.6	8.04
OR10–2	0.2	16.8	39.9	23.7	0	4	0.5	14.4	0.4	0.1	0	99.2	8.04
OR12–1	0.1	16.4	39.5	24.5	0	4	0.4	14.5	0.4	0.1	0	100.6	8.00
OR12–2	0.1	16	41.2	22.8	0	4	0.5	14.9	0.4	0.1	0	102.0	7.96
OR13–1	0.2	13.4	41.5	21.9	0	5.5	0.5	16.5	0.4	0.1	0	100.2	8.14
OR20–2	0.2	16.7	42.9	21.9	0	3.8	0.4	13.8	0.4	0.1	0	105.8	7.94
OR20–3	0.3	16	42.7	21.1	0.1	4	0.5	14.9	0.3	0	0	99.9	7.96
OR20–4	0.2	17.6	41.5	23.2	0	1.7	0.2	15.1	0.3	0	0	91.9	7.98
Clinopyroxene													
OR08–1	3.6	16.4	52.2	7.7	0.5	8.9	0.5	9.9	0.1	0.1	0	96.0	4.06
OR10–4	5.5	12.6	55.9	7.9	0.1	11.7	0.7	5.4	0.1	0.1	0	100.0	4.01
OR17–1	5.7	11.7	55.8	9.4	0.1	11.1	0.6	5.4	0.1	0.1	0	100.2	4.00
OR18–1	1.9	22	54.4	4	0.1	11.8	0.6	4.8	0.1	0.1	0.1	98.6	4.03
Titanite													
OR10–3	0	0	31.1	1.5	0	29	37.1	1	0.1	0	0	95.9	3.04

All totals are normalized to 100%, following the approach of Timmerman et al. (2015)

[a] The oxides are in wt%. The total sum of the different oxides is normalised to 100 wt%

[b] The original total in wt% before normalisation

[c] The total sum of cations (Cat) in atoms per formula unit (apfu) for 6 O for clinopyroxene, 12 O for garnet, and 5 O for titanite

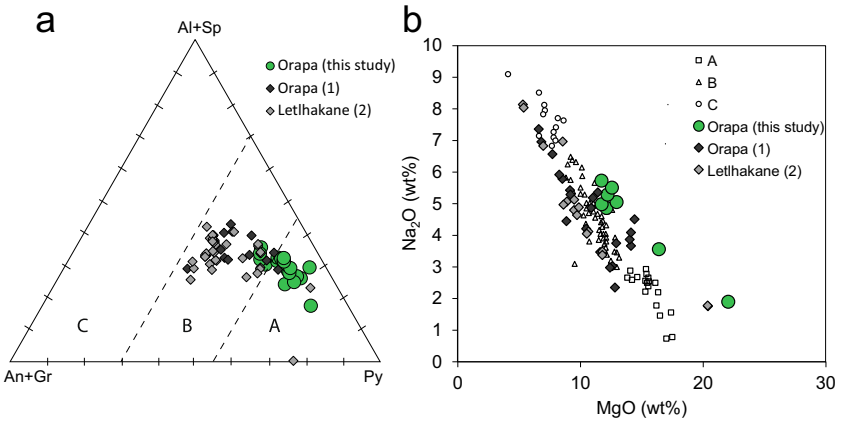

Fig. 4 **a** Orapa garnet end-member compositions were calculated with Fe^{2+}/Fe^{3+} separations based on Droop (1987) and plotted (green symbols; this study and Timmerman et al. 2017) on the eclogitic garnet classification diagram of Coleman et al. (1965). The studied garnet inclusions have relatively low Ca contents compared to inclusions from Orapa (1: dark grey symbols; Gurney et al. 1984) and Letlhakane (2: light grey symbols; Deines and Harris 2004). Al + Sp, Gr + An, Py stand for almandine+spessartine, grossular+andradite, pyrope. A, B, and C stand for garnet groups found in 'eclogites in kimberlites and ultramafic rocks', in 'high grade metamorphic rocks', and in 'amphibolites and granulites' respectively (Coleman et al. 1965). **b** Clinopyroxenes plotted on the Taylor and Neal (1989) classification diagram demonstrating that this suite is richer in Na and Mg compared to other eclogitic clinopyroxenes from Letlhakane (Deines and Harris 2004) and Orapa (Gurney et al. 1984)

in the studied diamonds therefore suggest either young diamond formation, mantle residence in a cool environment, and/or low aggregation rates due to low N concentrations. Given that most monocrystalline diamonds are Type IaAB, with A- and B-centres, the presence of relict unaggregated N in the studied diamonds is unusual. A dating study was previously performed on silicate inclusions derived from the colourless outer zones of these same unusual yellow Orapa diamonds and allows us to assess if the diamonds represent a young growth event. The inclusions yielded isochron ages of 140 ± 93, 1096 ± 230, and 1699 ± 340 Ma (Timmerman et al. 2017); given that the kimberlite eruption age is 93.1 Ma (Allsopp et al. 1989) these diamond ages indicate that most growth zones of the diamonds did not have a short mantle residence. Therefore, the relict unaggregated N does not appear related to extremely young diamond formation (i.e., <10 Ma before kimberlite eruption).

Diamond formation temperatures can be estimated from thermobarometric calculations using the compositions of included minerals assumed or proven to be in equilibrium. Nitrogen aggregation is, among other things, strongly dependent on temperature. Nitrogen concentrations and aggregation state can give time averaged mantle residence temperatures. The equilibration temperatures of 1080-1160 °C for three non-touching garnet-clinopyroxene pairs suggest that diamond formation did not occur at unusually low temperatures. It is possible, however, that diamond formation took place during a thermal perturbation associated with local intrusion of hot (asthenosphere derived) melts/fluids. Subsequent cooling to ambient mantle conditions would have resulted in a lower time averaged residence temperature for the diamonds. A similar idea was proposed for Namibian diamonds (Cartigny et al. 2004) to explain differences between mineral equilibration temperatures and residence temperatures calculated based on N systematics. Based on the N_s^0 (Table 1) and maximum A-centre contents (Electronic supplementary material 4), activation energies from Taylor et al. (1996), and the main mantle residence time of 1 Ga, an averaged mantle residence temperature would give 950–980 °C for cuboid sectors and 745–770 °C for octahedral sectors in this study. The diamond stability field is inferred to be at temperatures above 780–825 °C based on the geotherm beneath the Orapa field (Preston et al. 2012). Thus, it cannot be excluded that these diamonds resided for extended periods of time at relatively low temperatures in the diamond stability field, hence preserving small amounts of single N. It must be pointed out, however, that these diamond mantle residence temperatures are highly speculative, as aggregation states cannot be quantitatively calculated with such low N concentrations and with the presence of unknown defects in the one-phonon region. These residence temperatures and residence ages are, however, higher than proposed for Ib-IaA diamonds from Zimmi, West Africa (Smit et al. 2016).

The unaggregated N defects are considered mostly a consequence of the difficulty of aggregation at low N concentrations. The aggregation process for N concentrations of less than 200 at.ppm is very slow (Taylor et al. 1990). The aggregation of positively charged single N is even slower than neutral single N (Babich and Feigelson 2009), possibly explaining the relict N_s^+ (1332 cm^{-1} band) in the current study. In addition, Goss et al. (2014) suggested that H has the potential to modify the kinetics of N aggregation and may explain why N did not aggregate well beyond A-centres in the studied diamonds.

Origin of the diamond-forming fluid

Large differences in N content, C isotope composition and major element compositions of different inclusion parageneses in diamonds suggest that diamonds of various origins are sampled by individual kimberlites (see review in Stachel and Harris 2008). The major element compositions of the studied inclusions have mineral compositions that are within eclogitic fields in discrimination diagrams for garnets and clinopyroxenes (Fig. 4). Compared to previous studies of eclogitic diamonds from Orapa (Gurney et al. 1984; Deines et al. 1993; Deines and Harris 2004), the inclusions in the yellow diamonds are in general depleted in Ca, Fe, and Al, and enriched in Mg. Despite distinct differences in major element characteristics of different inclusion populations from Orapa, the mineral equilibration temperatures are essentially indistinguishable when using the same Fe-Mg exchange thermometer of Krogh (1988) at a pressure of 5 GPa: 1080–1160 °C for the unusual yellow Orapa diamonds and ~1080–1150 °C for other Orapa diamonds (Fig. 5; Deines and Harris 2004 and references therein). Thus, while all studied Orapa inclusions appear to have formed at similar temperatures from the diamond-forming fluids, the

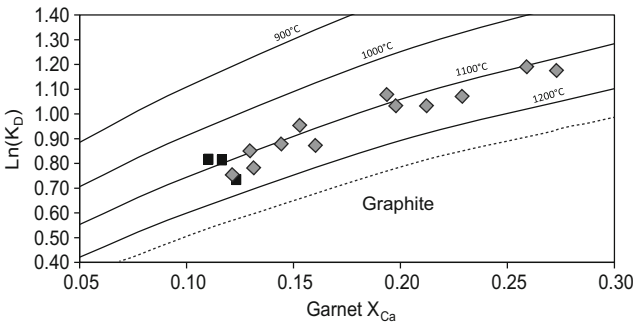

Fig. 5 Relationship between Mg/Fe partitioning of co-existing eclogitic garnet-clinopyroxene pairs ($K_D = (Fe/Mg)_{grt}/(Fe/Mg_{cpx})$) and mole fraction of Ca in garnet. Isotherms were calculated according to Krogh (1988) at a constant pressure of 5 GPa and the graphite-diamond transition was derived from Kennedy and Kennedy (1976). The studied Orapa diamonds (black squares) have similar mineral equilibration temperatures to previous studied Orapa diamonds (grey diamonds; Deines and Harris 2004 and references therein)

distinct N characteristics of the unusual yellow diamonds suggest these diamonds resided in a different environment, possibly at lower temperature (shallower) conditions than the majority of Orapa diamonds.

The limited range in C isotope ratios and N contents in the studied unusual yellow Orapa diamonds provides important constraints on their formation, as it suggests insignificant Rayleigh fractionation. Rayleigh fractionation modelling based on an N distribution coefficient of 2 (minimum Kd; Wiggers-de Vries et al. 2013b) and less than 20% relative depletion in N implies less than 20% of the fluid could have precipitated as diamond ($N/N_0 = f^{(Kn-1)}$). This implies diamond formation in a system that was not fluid-limited.

In summary, the morphology, growth structure of inner green luminescent and outer blue or non-luminescent zones, N concentration, inclusion major element composition, formation temperature, and C isotope composition of the yellow diamonds are all similar and indicate that the 20 studied complexly zoned diamonds formed by similar precipitation processes from comparable fluids. In combination with differences in trace element concentrations and Sr isotope compositions of the inclusions (Timmerman et al. 2017), the fluids that formed the outer colourless zones of the diamonds are likely to have resulted from mixing between depleted mantle and post-Archaean subducted sediment sources with a restricted range in C isotope compositions. It is, however, unclear in what time span the inner yellow and outer colourless zones have grown. Despite the uniform N concentration and C isotope composition of the inner and outer growth zones, a common resorption boundary (Electronic supplementary material 2) after the inner zone strongly supports multi-stage growth. The different isochron ages (~140, 1100, 1700 Ma; Timmerman et al. 2017) of the inclusions in the outer growth zone further support multiple episodes of growth. These data suggest that the diamonds formed over a long period of time, but currently it is unknown how long each diamond growth episode lasted. Was the same fluid activated several times for diamond growth or was there a new fluid with similar N-$\delta^{13}C$ characteristics injected to the growth environment? Further research is needed to determine diamond growth rates and the stability or reactivation of fluid compositions over long time periods.

Conclusion

The twenty studied diamonds from Orapa represent a previously undocumented eclogitic population. Their unusual yellow colour and related green luminescence in DiamondView™ images with sector growth zonation is distinct from other previously studied Orapa diamonds. The yellow colour appears to be, at least partially, associated with relict unaggregated N defects. The preservation of small amounts of N_s^+ and N_s^0 is mostly likely related to low N concentrations and possibly also to lower than normal mantle residence temperatures, that inhibited significant N aggregation beyond A-centres. The unaggregated N defects are not related to young diamond formation, as Sm-Nd isochron ages determined on silicate inclusions in the outer colourless zones are up to 1.7 Ga (Timmerman et al. 2017).

The inner yellow and outer colourless zones both have low total N concentrations (<50 at.ppm, except for the outer zone of OR02 at <125 at.ppm) and a relatively limited range in C isotope composition ($\delta^{13}C_{VPDB}$ values, −5.7 to −10.6‰). Garnet and clinopyroxene inclusions have an eclogitic composition with relatively low Ca and higher Mg contents compared to previous studies of diamonds from the Orapa cluster. Although diamond formation temperatures inferred from inclusion thermometry are similar to other Orapa diamonds, the unusual yellow diamonds possibly had lower time averaged mantle residence temperatures and form a distinct population.

Acknowledgments We thank Sergei Matveev and Susan Verdegaal-Warmerdam for their help with the EPMA and SIRMS analyses respectively. John Freeth of De Beers Technologies UK is thanked for laser cutting and polishing the diamond plates. Debswana is thanked for the generous provision of diamonds for this study. We thank two anonymous reviewers and editor Thomas Stachel for constructive comments that greatly improved the paper.

References

Allsopp HL, Bristow JW, Smith CB, Brown R, Gleadow AJW, Kramers JD, Garvie OG (1989) A summary of radiometric dating methods applicable to kimberlites and related rocks. In: Ross J, Jacques AL, Ferguson J, Green DH, O'Reilly SY, Danchin RV, Janse AJA (eds) Kimberlites and Related Rocks Volume 1. Proceedings of the Fourth International Kimberlite Conference. Geological Society of Australia Special Publication 14, Perth, Australia, pp. 343–357

Babich YV, Feigelson BN (2009) Distribution of N^+ centers in synthetic diamond single crystals. Inorg Mater 45:616–619

Boyd SR, Kiflawi I, Woods GS (1994) The relationship between infrared absorption and the A defect concentration in diamond. Philos Mag 69B:1149–1153

Cartigny P, Harris JW, Javoy M (1999) Eclogitic, peridotitic and metamorphic diamonds and the problems of carbon recycling—the case of Orapa (Botswana). In: The JB Dawson volume—Proceedings of the Seventh International Kimberlite Conference, Cape Town. Red Roof Design, Cape Town, pp 117–124

Cartigny P, Stachel T, Harris JW, Javoy M (2004) Constraining diamond metasomatic growth using C- and N-stable isotopes: examples from Namibia. Lithos 77:359–373

Clark CD, Davey ST (1984) One-phonon infrared absorption in diamond. J Phys C Solid State 17:1127–1140

Coleman RG, Lee DE, Beatty LB, Brannock WW (1965) Eclogites and eclogites: their differences and similarities. Geol Soc Am Bull 76: 483–508

Collins AT, Mohammed K (1982) Optical studies of vibronic bands in yellow luminescing natural diamonds. J Phys C Solid State 15:147–158

Deines P, Harris JW (2004) New insights into the occurrence of ^{13}C-depleted carbon in the mantle from two closely associated kimberlites: Letlhakane and Orapa, Botswana. Lithos 77:125–142

Deines P, Harris JW, Robinson DN, Gurney JJ, Shee SR (1991) Carbon and oxygen isotope variations in diamond and graphite eclogites from Orapa, Botswana, and the nitrogen content of their diamonds. Geochim Cosmochim Ac 55:515–524

Deines P, Harris JW, Gurney JJ (1993) Depth related carbon isotope and nitrogen concentration variability in the mantle below the Orapa kimberlite, Botswana, Africa. Geochim Cosmochim Ac 57:2781–1796

Deines P, Stachel T, Harris JW (2009) Systematic regional variations in diamond carbon isotopic composition and inclusion chemistry beneath the Orapa kimberlite cluster, in Botswana. Lithos 112:776–784

Droop GTR (1987) A general equation for estimating Fe^{3+} concentrations in ferromagnesian silicates and oxides from microprobe analyses, using stoichiometric criteria. Mineral Mag 51:431–435

Evans T, Qi Z (1982) The kinetics of the aggregations of nitrogen atoms in diamond. P Roy Soc Lond A Mat 381:159–178

Fritsch E (1998) The nature of color in diamonds. The Nature of Diamonds. Cambridge University Press, Cambridge, pp 23–47

Goss JP, Briddon PR, Hill V, Jones R, Rayson MJ (2014) Identification of the structure of the 3107 cm^{-1} H-related defect in diamond. J Phys-Condens Mat 26:145801–145806

Gress MU, Timmerman S, van den Heuvel Q, Schulten E, Chinn IL, Davies GR (2017) Variation in diamond growth events recorded in Botswanan diamonds. 11IKC extended abstract#4509

Gurney JJ, Harris JW, Rickard RS (1984) Silicate and oxide inclusions in diamonds from the Orapa Mine, Botswana. In: J. Kornprobst (Ed.), Kimberlites II: the mantle and crust–mantle relationships, Elsevier, Amsterdam, Dev Petrol 11:3–9

Hainschwang T, Fritsch E, Notari F, Rondeau B (2012) A new defect center in type Ib diamond inducing one phonon infrared absorption: the Y center. Diam Relat Mater 21:120–126

Kennedy CS, Kennedy GC (1976) The equilibrium boundary between graphite and diamond. J Geophys Res 81:2467–2470

Kiflawi I, Mayer AE, Spear PM, Van Wyk JA, Woods GS (1994) Infrared absorption by single nitrogen and A defect centres in diamond. Philos Mag 69B:1141–1147

King JM, Shigley JE, Gelb TH, Guhin SS, Hall M, Wang W (2005) Characterization and grading of natural-colour yellow diamonds. Gems Gemol 41:88–115

Kirkley MB, Gurney JJ, Otter ML, Hill SJ, Daniels LR (1991) The application of C isotope measurements to the identification of the sources of C in diamonds: a review. Appl Geochem 6:477–494

Klein-BenDavid O, Izraeli ES, Hauri E, Navon O (2004) Mantle fluid evolution—a tale of one diamond. Lithos 77:243–253

Krogh EJ (1988) The garnet-clinopyroxene Fe-Mg geothermometer - a reinterpretation of existing experimental data. Contrib Mineral Petrol 99:44–48

Lawson SC, Fisher D, Hunt DC, Newton ME (1998) On the existence of positively charged single-substitutional nitrogen in diamond. J Phys-Condens Mat 10:6171–6180

Liggins S (2010) Identification of point defects in treated single crystal diamond. Doctoral dissertation, University of Warwick, pp 241

Mendelssohn MJ, Milledge HJ (1995) Geologically significant information from routine analysis of the mid-infrared spectra of diamonds. Int Geol Rev 37:95–110

Meulemans TM, Borst AM, Davidheiser B, Davies GR. (2012) The origin and modification of the sub-continental lithospheric mantle of Botswana: constraints from peridotite xenoliths of the Orapa mine Botswana. 10IKC extended abstract#351

Navon O, Hutcheon ID, Rossman GR, Wasserburg GJ (1988) Mantle-derived fluids in diamond micro-inclusions. Nature 335:784–789

Petts DC, Stachel T, Stern RA, Hunt L, Fomradas G (2016) Multiple carbon and nitrogen sources associated with the parental mantle fluids of fibrous diamonds from Diavik, Canada, revealed by SIMS microanalysis. Contrib Mineral Petrol 171:1–15

Preston RP, Perritt SH, Seller MH, Wyatt BA (2012) Lithospheric structure beneath the Cretaceous Orapa kimberlite field, Botswana: 4D lithosphere imaging using garnet indicator mineral chemistry. 10IKC extended abstract#312

Schrauder M, Navon O (1994) Hydrous and carbonatitic mantle fluids in fibrous diamonds from Jwaneng, Botswana. Geochim Cosmochim Ac 58:761–771

Shee SR (1978) The mineral chemistry of xenoliths from the Orapa kimberlite pipe, Botswana. Unpublished M.Sc. thesis, University of Cape Town, Cape Town, pp 148

Shirey SB, Cartigny P, Frost DJ, Keshav S, Nestola F, Nimis P, Pearson DG, Sobolev NV, Walter MJ (2013) Diamonds and the geology of mantle carbon. In: Hazen RM, Jones AP, Baross JA (eds) Carbon in Earth. Rev Mineral Geochem, vol 75. Miner Soc Am, Chantilly, pp 355–421

Smit KV, Shirey SB, Wang W (2016) Type Ib diamond formation and preservation in the West African lithospheric mantle: Re–Os age constraints from sulphide inclusions in Zimmi diamonds. Precambrian Res 286:152–166

Stachel T, Harris JW (2008) The origin of cratonic diamonds - Constraints from mineral inclusions. Ore Geol Rev 34:5–32

Stachel T, Viljoen KS, McDade P, Harris JW (2004) Diamondiferous lithospheric roots along the western margin of the Kalahari Craton - the peridotitic inclusion suite in diamonds from Orapa and Jwaneng. Contrib Mineral Petrol 147:32–47

Taylor LA, Neal CR (1989) Eclogites with oceanic crustal and mantle signatures from the Bellsbank kimberlite, South Africa, Part I: mineralogy, petrography, and whole rock chemistry. J Geol 97:551–567

Taylor WR, Jaques AL, Ridd M (1990) Nitrogen-defect aggregation characteristics of some Australasian diamonds: time-temperature constraints on the source regions of pipe and alluvial diamonds. Am Mineral 75:1290–1310

Taylor WR, Canil D, Milledge HJ (1996) Kinetics of Ib to IaA nitrogen aggregation in diamond. Geochim Cosmochim Ac 60:4725–4733

Timmerman S, Matveev S, Gress MU, Davies GR (2015) A methodology for wavelength dispersive electron probe microanalysis of unpolished silicate minerals. J Geochem Explor 159:243–251

Timmerman S, Koornneef JM, Chinn IL, Davies GR (2017) Dated eclogitic diamond growth zones reveal variable recycling of crustal carbon through time. Earth Planet Sc Lett 463:178–188

Welbourn CM, Cooper M, Spear PM (1996) De Beers natural versus synthetic diamond verification instruments. Gems Gemol 32: 156–169

Wiggers-de Vries DF (2013) Origin and evolution of Yakutian diamonds: constraints on sources and timing from a combined petrological and geochemical study of diamonds and their inclusions. Doctoral dissertation, VU University Amsterdam, pp. 275

Wiggers-de Vries DF, Pearson DG, Bulanova GP, Smelov AP, Pavlushin AD, Davies GR (2013a) Re–Os dating of sulphide inclusions zonally distributed in single Yakutian diamonds: Evidence for multiple episodes of Proterozoic formation and protracted timescales of diamond growth. Geochim Cosmochim Ac 120:363–394

Wiggers-de Vries DF, Bulanova GP, De Corte K, Pearson DG, Craven JA, Davies GR (2013b) Micron-scale coupled carbon isotope and nitrogen abundance variations in diamonds: evidence for episodic diamond formation beneath the Siberian Craton. Geochim Cosmochim Ac 100:176–199

Woods GS, Collins AT (1983) Infrared absorption spectra of hydrogen complexes in type I diamonds. J Phys Chem Solids 44:471–475

Zedgenizov DA, Kalinina VV, Reutsky VN, Yuryeva OP, Rakhmanova MI (2016) Regular cuboid diamonds from placers on the northeastern Siberian platform. Lithos 265:125–137